

## SPATIAL DISTRIBUTION OF EMBEDDED CLUSTERS IN THE ROSETTE MOLECULAR CLOUD: IMPLICATIONS FOR CLUSTER FORMATION

RANDY L. PHELPS<sup>1</sup>

Observatories of the Carnegie Institution of Washington, 813 Santa Barbara Street, Pasadena, CA 91101; phelps@ociw.edu

AND

ELIZABETH A. LADA<sup>1,2,3</sup>

University of Maryland, Department of Astronomy, College Park, MD 20742; lada@astro.umd.edu

Received 1996 May 24; accepted 1996 September 23

### ABSTRACT

We have imaged a  $\sim 0.7$  deg<sup>2</sup> region of the Rosette Molecular Cloud (RMC) using the simultaneous quad infrared imaging device on the Kitt Peak National Observatory 1.3 m telescope. The region observed covers most of the <sup>13</sup>CO emission detected by Blitz & Stark, as well as the majority of the *IRAS* point sources listed by Cox, Deharveng, & Leene and Williams, Blitz, & Stark. In this paper, we report the detection of seven young embedded clusters in the RMC, five of which were previously unknown.

All seven clusters are associated with *IRAS* sources and with molecular (<sup>13</sup>CO) clumps (Williams et al.), although not all *IRAS* sources or molecular clumps are associated with clusters. The molecular clumps that contain clusters are among the most massive clumps in the cloud, indicating that high-mass regions are required for the formation of clusters. However, the majority of massive <sup>13</sup>CO clumps in the RMC are not associated with embedded clusters, suggesting that conditions other than high mass, such as high density, are needed for cluster formation.

The spatial location of most of the clusters suggests that cluster formation may be triggered by the ionization fronts from the nearby H II region associated with NGC 2244. However, triggered star formation cannot explain the presence of all of the clusters, suggesting that more than one mechanism may be at work forming clusters in this cloud.

*Subject headings:* ISM: clouds — ISM: individual (Rosette) — ISM: molecules — open clusters and associations: general — stars: formation

### 1. INTRODUCTION

Over the past several years, near-infrared imaging observations of star-forming regions have revealed the existence of a large number of young embedded clusters (e.g., Lada, Strom, & Myers 1993; Zinnecker et al. 1993). To date, however, only a few large-scale, systematic surveys for embedded objects within molecular clouds have been completed (i.e., L1630, Lada et al. 1991; L1641, Strom, Strom, & Merrill 1993; IC 5146, Lada et al. 1994; Lada, Lada, & Bally 1996; Taurus, Gomez et al. 1993). Such surveys provide unique databases for investigations of the general problems of star formation. In particular, they can be used to study the distribution of star formation within molecular clouds and address the following questions: (1) Which modes of star formation (clustered or isolated) are present and/or dominate? (2) Is star formation triggered or does it occur spontaneously? (3) What are the environments under which stars of various masses form. Furthermore, these surveys, in combination with molecular, atomic, and *IRAS* surveys of the distribution of gas and dust in molecular clouds provide powerful tools with which to probe the conditions needed for stellar birth.

An ideal molecular cloud in which to perform such a survey is the Rosette Molecular Cloud (RMC). The RMC, located at a distance of 1600 pc (e.g., Perez, The, & West-

erlund 1987) in the constellation of Monoceros, sits at the edge of an ionization front created by the stars within the optically revealed cluster NGC 2244, and it contains several known *IRAS* point sources (Cox, Deharveng, & Leene 1990). It has been used as an example of possible triggered star formation (Cox et al. 1990), although the evolutionary status of the embedded sources remains unknown. The RMC has been extensively mapped in CO (Blitz & Thaddeus 1980), <sup>13</sup>CO (Blitz & Stark 1986), H I (Kuchar & Bania 1993), and in the mid-infrared with *IRAS* (Cox et al. 1990), so the large-scale properties of the gas and dust in the region are well studied.

We have completed a large-scale, systematic near-infrared imaging survey of the RMC covering the majority of the <sup>13</sup>CO emission detected by Blitz & Stark (1986). The ultimate objective of this survey is to establish the number, location, and evolutionary status of the stars in this cloud. When combined with the existing studies of the gas and dust, these data provide a comprehensive view of the conditions for star formation in this region. In this paper, we present the initial results of the survey, the detection of seven embedded clusters in the RMC, as well as an investigation of the correlations between the distribution of embedded clusters and the distribution of *IRAS* sources and molecular clumps in the cloud.

### 2. OBSERVATIONS

Observations were made over the period 1994 January 5–10 with the recently decommissioned Kitt Peak National Observatory (KPNO) 1.3 meter telescope and the simultaneous quad infrared imaging device (SQIID). SQIID con-

<sup>1</sup> Visiting Astronomer, Kitt Peak National Observatory. KPNO is operated by AURA, Inc., under contract to the National Science Foundation.

<sup>2</sup> Hubble Fellow.

<sup>3</sup> Current address: University of Florida, Department of Astronomy, 211 SSRB, Gainesville, FL 32611.

tains four  $256 \times 256$  platinum silicide (PtSi) focal plane arrays. Dichroic mirrors allow simultaneous images to be taken in the  $J$  ( $1.2 \mu\text{m}$ ),  $H$  ( $1.6 \mu\text{m}$ ),  $K$  ( $2.2 \mu\text{m}$ ), and  $L$  ( $3.4 \mu\text{m}$ ) passbands, covering a field of  $\sim 5'.5 \times 5'.5$  with a resolution of  $1''.36 \text{ pixel}^{-1}$  at  $K$ -band. For these reasons, the 1.3 m telescope/SQIID combination was uniquely suited for large-scale near-infrared surveys.

For this observing program, only the  $J$ ,  $H$ , and  $K$  frames were saved. Over the course of the 6 night run, we obtained images of 155 contiguous fields toward the RMC, covering an area of approximately  $0.7 \text{ deg}^2$ . The region that we observed contained most of the  $^{13}\text{CO}$  emission mapped by Blitz & Stark (1986), 17 of the *IRAS* sources cataloged by Cox et al. (1990), and nine of the *IRAS* sources listed by Williams, Blitz, & Stark (1995, hereafter WBS95). In addition, we observed 10 control fields ( $\sim 0.08 \text{ deg}^2$ ) off the molecular cloud in order to estimate the contamination of our sample by field stars. The images were dark-subtracted and flat-fielded in a manner similar to that of Lada & Lada (1995). A detailed discussion of the observations and data analysis will be presented in a forthcoming paper.

### 3. RESULTS

#### 3.1. Clusters

For the initial analysis of our RMC data set, a visual inspection of the images was independently undertaken by each of us in order to look for possible clusterings of stars (defined as apparent enhancements over the local density of field stars). This resulted in identification of seven embedded clusters. Figure 1 presents our  $K$ -band images of these seven clusters. Figures 1*a*–1*e* are composed of single SQIID frames, while Figures 1*f* and 1*g* are made up of  $2 \times 2$  mosaics. Two of the embedded clusters, numbers 3 and 4 (see Table 1 for cluster identification numbers and positions), have been previously identified by earlier near-

infrared imaging studies (cluster 3, Carpenter et al. 1993; cluster 4, Block, Geballe, & Dyson 1993; Hanson et al. 1993; Phelps 1994). The remaining five embedded clusters are newly identified, although many of these positions had been previously recognized as regions of recent star formation.

The clusters are not visible on the Palomar Observatory Sky Survey (POSS) images. In the near-infrared images, the clusters have apparent diameters of roughly  $1' - 2'$ , which, at the 1600 pc distance of the RMC (Perez et al. 1987), corresponds to a linear diameter of  $0.5 - 1 \text{ pc}$ . These sizes are similar to those determined for other young, nearby, embedded clusters (e.g., Lada & Lada 1991). Together these observations indicate that the clusters are indeed young and still embedded in their parental cloud.

Figure 2 shows the locations of the embedded clusters (*circles*) and the Cox et al. (1990) *IRAS* sources (*stars*) relative to the distribution of CO (Blitz & Stark 1986) in the RMC. The Rosette Nebula has an optical extent of  $\sim 40'$  on the POSS prints, so that the maximum extent of the nebula coincides with the large arc seen in the CO map at  $206^\circ 2 \leq l \leq 207^\circ$ . Figure 3 shows the location of the embedded clusters (*circles*) relative to the distribution of  $^{13}\text{CO}$  in the region, as well as the ionized gas in the Rosette Nebula.

#### 3.2. Association with *IRAS* Sources

The distribution of embedded clusters was compared to the distribution of *IRAS* sources found in the RMC (Fig. 2). All seven embedded clusters are associated with *IRAS* sources, however, not all *IRAS* sources in the cloud are associated with clusters. In fact, 10 *IRAS* sources that were identified by Cox et al. (1990) and covered by our near-infrared (NIR) survey do not show any evidence of clustering.

WBS95 used more restrictive criteria for the selection of *IRAS* sources with color indices of typical star-forming

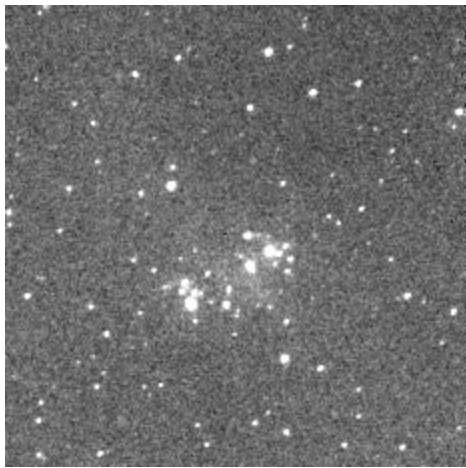
TABLE 1  
PROPERTIES OF *IRAS* SOURCES IN THE ROSETTE MOLECULAR CLOUD<sup>a</sup>

Cluster Number	<i>IRAS</i> Name	R.A. <sup>b</sup> (1950)	Decl. <sup>c</sup> (1950)	Longitude	Latitude	$F_\nu$ (Jy)				Luminosity ( $L_\odot$ )
						12 $\mu\text{m}$	25 $\mu\text{m}$	60 $\mu\text{m}$	100 $\mu\text{m}$	
With Clusters										
1	06291+0421	06 29 09.3	04 21 44	206.84	-2.38	8.4	21.4	252.6	498.8	2810
2	06306+0437	06 30 37.3	04 37 16	206.78	-1.94	3.0	11.9	88.5	247.2	1222
3	06308+0402	06 30 52.7	04 02 27	207.33	-2.15	13.3	38.3	602.6	949.0	5795
4	06314+0427	06 31 26.6	04 27 17	207.02	-1.83	6.1	6.5	129.3	323.6	5310
5	06318+0420	06 31 53.6	04 20 13	207.18	-1.79	1.5	3.8	36.6	995.2	...
6	06319+0415	06 31 59.0	04 15 09	207.27	-1.81	78.4	375.8	958.8	995.2	12400
7	06329+0401	06 32 54.1	04 01 21	207.58	-1.71	0.4	0.9	4.9	12.2	72
Without Cluster										
...	06294+0352	06 29 29.0	03 52 22	207.31	-2.54	1.4	4.4	30.0	43.9	323
...	06298+0430	06 29 53.7	04 30 10	206.80	-2.15	0.3	1.9	29.1	101.0	...
...	06314+0421	06 31 28.1	04 21 26	207.11	-1.87	0.7	1.6	105.0	323.6	...
...	06315+0438	06 31 31.6	04 38 31	206.87	-1.73	1.1	1.5	27.3	118.3	467
...	06316+0432	06 31 36.9	04 32 48	206.96	-1.75	0.5	0.6	5.3	323.6	...
...	06318+0441	06 31 49.6	04 41 12	206.86	-1.64	0.7	0.9	9.8	73.9	...
...	06320+0438	06 32 01.7	04 38 37	206.92	-1.62	1.7	3.6	16.7	85.1	372
...	06322+0427	06 32 16.5	04 27 40	207.11	-1.65	0.4	0.7	10.2	73.9	...
...	06325+0354	06 32 31.3	03 54 14	207.64	-1.85	0.7	2.5	27.2	67.0	335
...	06327+0423	06 32 47.0	04 23 13	207.24	-1.57	0.5	0.8	8.2	62.7	220

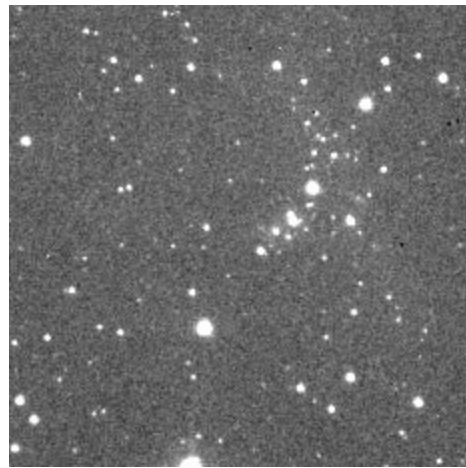
<sup>a</sup> Adapted from Cox et al. 1990.

<sup>b</sup> Right ascension is in units of hours, minutes, and seconds.

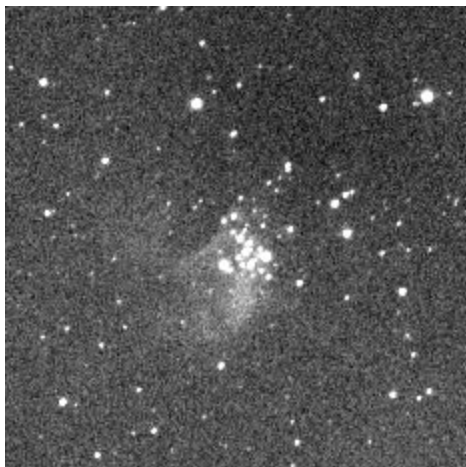
<sup>c</sup> Declination is in units of degrees, arcminutes, and arcseconds.



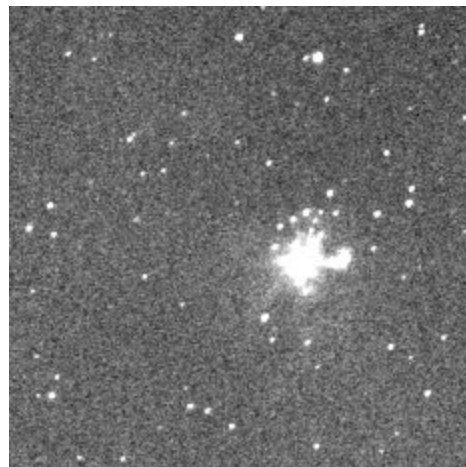
(a) Cluster 1



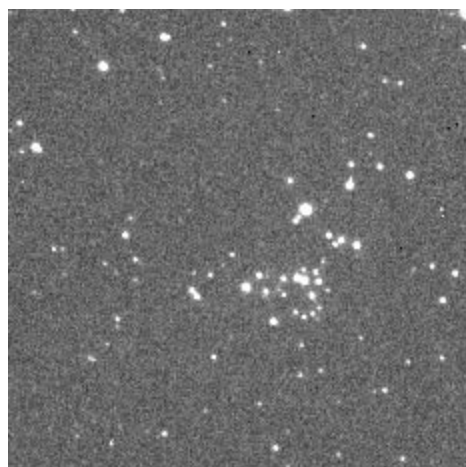
(b) Cluster 2



(c) Cluster 3

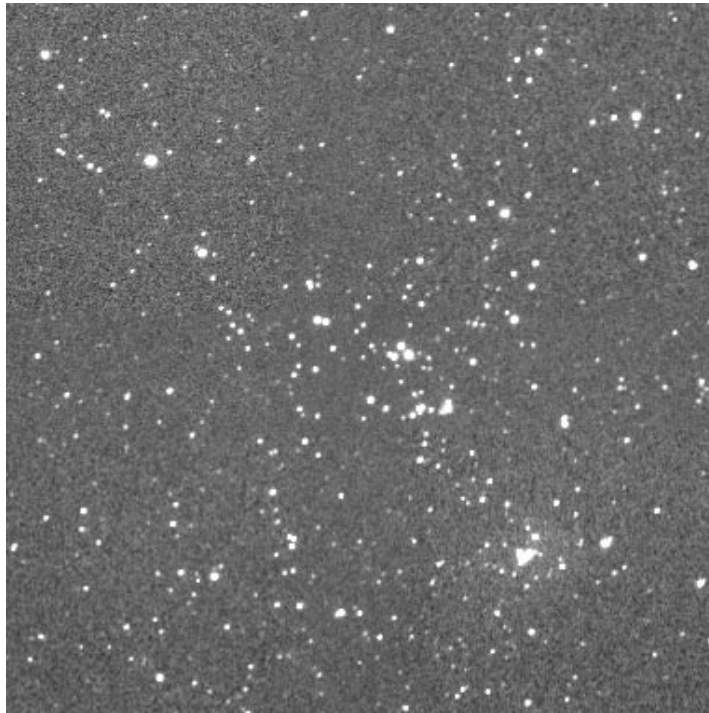


(d) Cluster 6



(e) Cluster 7

FIG. 1.—*K*-band images of the embedded clusters. Figs. 1*a*–1*e* are single-frame SQUID images, 5/5 on a side. Figs. 1*f* and 1*g* are 2 × 2 mosaics, covering 11' on a side. These data were taken in an equatorial reference frame. North is up and east is to the left. Fig. 1*a*, cluster 1; Fig. 1*b*, cluster 2; Fig. 1*c*, cluster 3; Fig. 1*d*, cluster 6; Fig. 1*e*, cluster 7; Fig. 1*f*, cluster 4; Fig. 1*g*, cluster 5. The position of the *IRAS* source associated with cluster 4 (*IRAS* 06314 + 0427) is located in the lower right-hand portion of Fig. 1*g*, and it coincides with the small clump of stars surrounded by faint nebulosity (Block et al. 1993); although a more distributed population of stars, perhaps representing a larger cluster of stars, is also seen in this region.



(f) Cluster 4



(g) Cluster 5

FIG. 1—*Continued*

regions. Their criteria, similar to those of Cox et al. (1990), but requiring more detailed color information and reliably measured fluxes, result in a smaller subset of *IRAS* sources with characteristics of star-forming regions. Examination of their list reveals that six out of the nine WBS95-selected

*IRAS* sources within our survey boundaries are associated with six of the seven embedded RMC clusters, indicating that their criteria result in a good prediction of the presence of embedded clusters.

Table 1 summarizes the properties of the Cox et al. (1990)

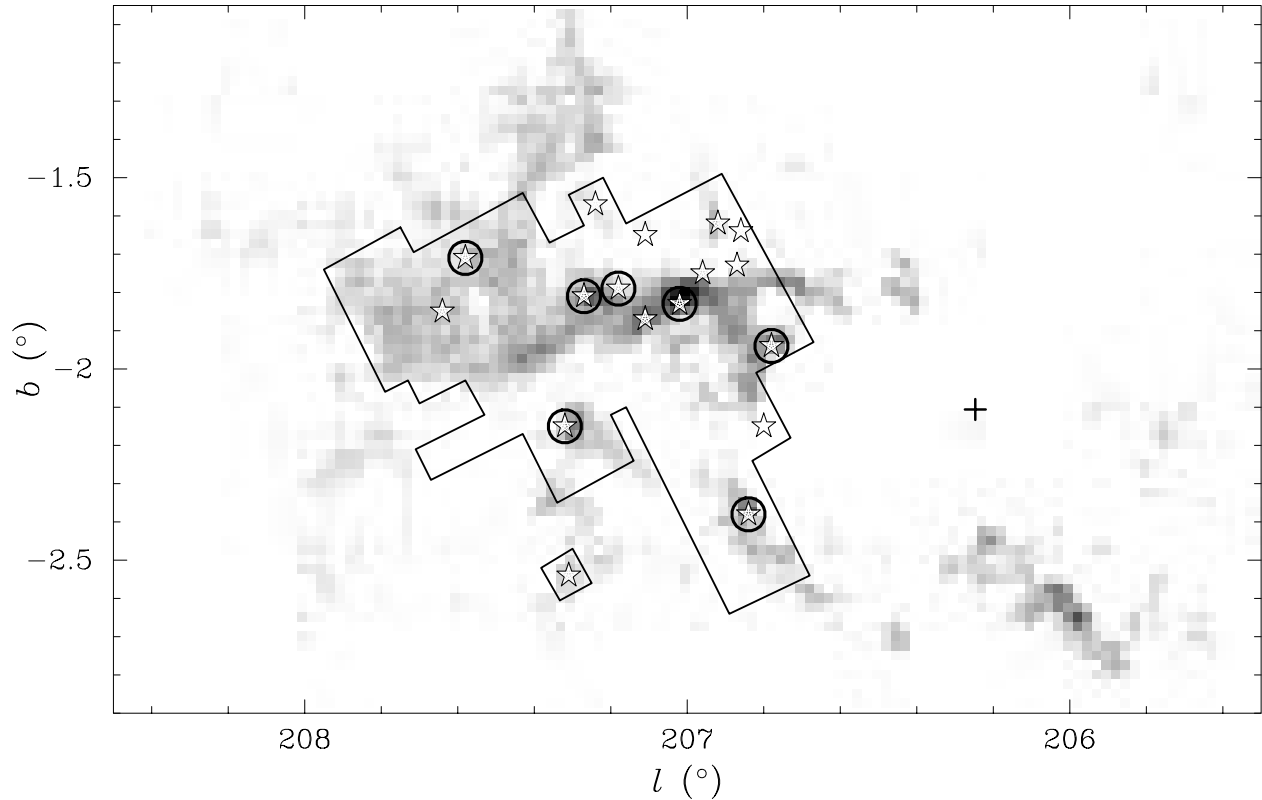


FIG. 2.— $^{12}\text{CO}$  map of the Rosette Molecular Cloud from Blitz & Stark (1986), as presented in Williams et al. (1995). Stars indicate the locations of *IRAS* sources (Cox et al. 1990), while circles indicate the locations of embedded clusters. The cross indicates the center of the optical nebula of the Rosette Nebula. CO map courtesy of Jonathan Williams. Outline encompasses the region observed during the SQIID near-infrared survey.

*IRAS* sources that are located within our survey boundaries. Positions, *IRAS*  $12\ \mu\text{m}$ ,  $25\ \mu\text{m}$ ,  $60\ \mu\text{m}$ , and  $100\ \mu\text{m}$  fluxes, and source luminosities (for high-quality detections), adapted from Cox et al. (1990) are listed. The *IRAS* sources are divided into two groups, those with clusters and those without. The luminosities and  $12\ \mu\text{m}$ ,  $25\ \mu\text{m}$ , and  $60\ \mu\text{m}$  fluxes are higher for sources associated with clusters than for those without clusters.

### 3.3. Association with CO Peaks

Recently, WBS95 analyzed the clumpy structure of the

TABLE 2  
*IRAS* SOURCES:  $^{13}\text{CO}$  CLUMP MASSES<sup>a</sup>

Cluster	<i>IRAS</i>	Clump	$M_{\text{LTE}}$	$M_{\text{grav}}$	$\alpha$	$L/L_{\odot}$
With Clusters						
1	06291+0421	11	847	602	1.4	2810
2	06306+0437	18	452	252	1.8	1222
3	06308+0402	7	1175	444	2.6	5795
4	06314+0427	1	2532	674	3.8	5310
5	06318+0420	19	407	282	1.4	
6	06319+0415	2	2417	1160	2.1	12400
7	06329+0401	3	2373	1572	1.5	72
Without Clusters						
...	06314+0421	17	467	359	1.3	
...	06320+0438	32	150	263	0.6	372
...	06322+0427	50	56	99	0.6	
...	06325+0354	5	1700	1011	1.7	335
...	06327+0423	20	372	967	0.4	220

<sup>a</sup> From WBS95 and Cox et al. 1990.

molecular gas in the RMC as traced by CO and  $^{13}\text{CO}$  observations (Blitz & Thaddeus 1980; Blitz & Stark 1986). WBS95 identified and studied the properties of 70 clumps of gas in the cloud using an automated clump finding routine. In an attempt to investigate the relationship between the embedded clusters and their parental molecular gas, we have compared the locations of the seven embedded clusters to the distribution of the WBS95 molecular clumps in the RMC. We find that all seven clusters are associated with massive  $^{13}\text{CO}$  clumps ( $M > 200 M_{\odot}$ ). Specifically, the clusters lie within clump boundaries based on the derived radii of the clumps determined in WBS95. This result is summarized in Table 2, which lists the cluster IDs, associated *IRAS* sources, associated molecular clump mass, and *IRAS* luminosity. Table 2 also lists clumps associated with non-cluster *IRAS* sources. The clump masses are from WBS95, and they were determined both by assuming local thermodynamic equilibrium from the available  $^{12}\text{CO}$  and  $^{13}\text{CO}$  data ( $M_{\text{LTE}}$ ), and by calculating a mass,  $M_{\text{grav}}$ , for which the internal motions within a clump are bound by gravity. The *IRAS* luminosities are from Cox et al. (1990).

The clumps associated with embedded clusters are among the most massive clumps identified in the RMC by WBS95 and are, on average, more massive than clumps associated with noncluster *IRAS* sources. Although all seven embedded clusters are associated with massive  $^{13}\text{CO}$  clumps, not all massive  $^{13}\text{CO}$  clumps are associated with embedded clusters. Comparison of the WBS95 catalog with our NIR survey reveals that  $\sim 20$ – $40$  massive  $^{13}\text{CO}$  clumps (depending on whether you consider the LTE or gravitational mass, respectively) do not appear to have recognizable embedded clusters.

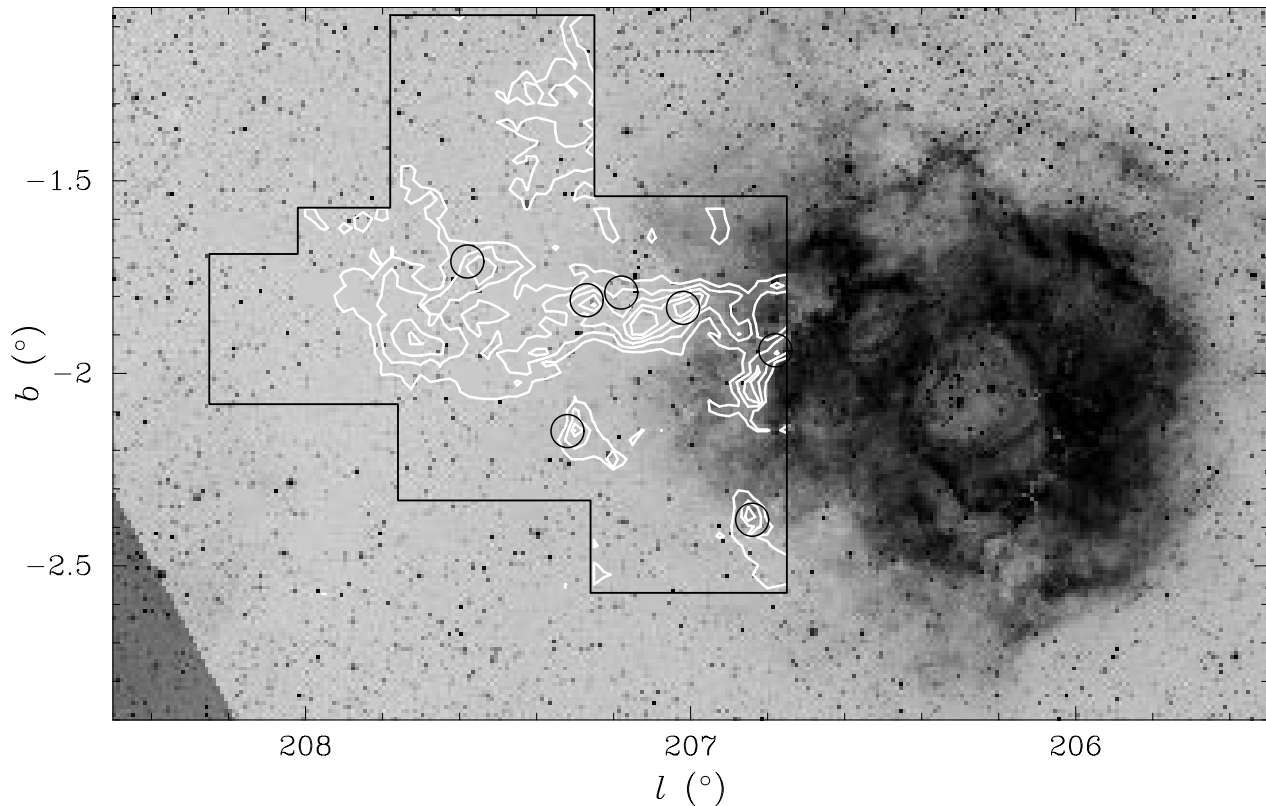


FIG. 3.—Digital sky survey image of the Rosette region. Circles indicate the locations of the embedded clusters.  $^{13}\text{CO}$  contour map from Blitz & Stark (1986) is overlaid—the outline indicates the region of their  $^{13}\text{CO}$  survey. The Rosette image is based on photographic data obtained using the UK Schmidt Telescope. The UK Schmidt Telescope was operated by the Royal Observatory Edinburgh, with funding from the UK Science and Engineering Research Council, until 1988 June, and thereafter by the Anglo-Australian Observatory. Original plate material is the copyright of the Royal Observatory Edinburgh and the Anglo-Australian Observatory. Plates were processed into the present compressed digital form with their permission. The Digitized sky survey was produced at the Space Telescope Science Institute.

#### 4. DISCUSSION

The initial analysis of our *JHK* survey data for the RMC reveals seven embedded clusters of stars, all of which are associated with  $^{13}\text{CO}$  peaks and *IRAS* sources. The presence of such a large number of clusters indicates that clustering is an important mode of star formation in the RMC, a result consistent with findings in other molecular clouds (e.g., L 1630, Lada et al. 1991; Taurus, Gomez et al. 1993; L 1641 Strom et al. 1993; IC 5146, Lada, Lada, & Bally 1996). The extent to which clustering in the RMC is the *dominant* mode of star formation, as is found in the L 1630 cloud (Lada et al. 1991), will be addressed in a subsequent paper.

Our observation that the RMC embedded clusters are associated with the most massive molecular clumps indicates that high-mass regions are required for the formation of clusters. However, the lowest mass clumps associated with clusters have  $M_{\text{LTE}} \sim 400 M_{\odot}$  ( $M_{\text{grav}} \sim 250 M_{\odot}$ ), meaning that 63% (85% using  $M_{\text{grav}}$ ) of the clumps with a mass this great or higher do not contain clusters. Since the majority of the massive  $^{13}\text{CO}$  clumps in the RMC do not contain embedded clusters, high mass cannot be the only condition needed for cluster formation. Indeed, comparison of the surveys for near-infrared sources and for dense CS(2–1) molecular gas ( $n > 10^4 \text{ cm}^{-3}$ ) in the L1630 cloud has shown that both high mass and high gas density are needed to form embedded clusters (Lada 1992). Further-

more, a detailed study of the properties of massive CS cores in L1630 suggests that cores forming rich clusters contain a higher fraction of gas with  $n > 10^5 \text{ cm}^{-3}$  than CS cores exhibiting substantially lower star formation efficiencies (Lada, Evans, & Falgarone 1996). Consequently, the large number of massive yet clusterless  $^{13}\text{CO}$  cores in the RMC may be the result of these cores having insufficient densities. This is supported by the observation that three of the  $^{13}\text{CO}$  clumps associated with clusters in the RMC appear to be “supervirial,” having  $\alpha \geq 2$  (Table 2), where  $\alpha$  is the ratio of the clump self gravity over the total clump kinetic energy, given by  $M_{\text{LTE}}/M_{\text{grav}}$  (WBS95). This condition can be interpreted as evidence that these clumps may have higher densities than is traced by the  $^{13}\text{CO}$  observations. To test this, observations of the massive RMC cores in a tracer that is sensitive to volume density such as CS or  $\text{NH}_3$  are needed.

The nearby OB association, NGC 2244, provides a ready source of stellar winds, giving rise to an expanding H I shell that is spatially coincident with the edge of the RMC (Kuchar & Bania 1993). Is it possible that the cluster formation we observe in the RMC has been triggered by NGC 2244? It is already known that there are at least three sub-associations in the Mon OB2 complex, with diameters decreasing from 280 pc for the oldest to about 25 pc for NGC 2244 (Blaauw 1964), suggesting that sequential star formation has occurred on a larger scale. Examination of the spatial distribution of the embedded clusters (Figs. 2 and 3) may provide insights into the the star-forming

mechanisms at work within RMC itself. A large fraction of the young clusters are located in the western half of the cloud, in the direction toward NGC 2244, indicating that the environment in this region is conducive to cluster formation. It may be possible that the higher densities within these clumps, which are needed for the formation of embedded clusters, are achieved as a result of compression induced by the H II region. In particular, the lowest longitude clusters (numbers 1, 2, and 4) are located within or at the edge of the ionization front associated with the Rosette Nebula (Fig. 3). This strongly suggests that the formation of at least these three clusters has been triggered by NGC 2244 in a manner similar to that suggested in the sequential star formation models of Elmegreen & Lada (1977).

Blitz & Stark (1986) proposed a model of the RMC that included groups of high-density clumps embedded in an extended, low-density molecular gas. Inhomogeneities in the molecular material have been traced by Block (1990) using optical images. It is possible that inhomogeneities in the RMC may allow ultraviolet photons to penetrate deeper into the cloud, with the increase in pressure following the ionization of the low-density molecular gas giving rise to the collapse of the molecular clumps. Triggered formation of clusters 3, 5, and 6 might then result as well. Indeed, the presence of *IRAS* sources associated with cometary globules near clusters 4, 5, and 6 (Block, Dyson, & Madsen 1992; Patel, Xie, & Goldsmith 1993) provides evidence that inhomogeneities deep within the cloud may allow triggered star formation to occur.

Despite this evidence, however, it is doubtful that triggered star formation can account for the formation of all of the clusters in the RMC. While the majority of the clusters are not far from the Rosette Nebula ionization front, cluster 7 is most likely too far away from the Rosette H II region and the other embedded clusters to be explained by triggered star formation. An alternative could be that star formation in the RMC occurs spontaneously in the midplane, forming clusters 2, 4, 5, 6, and 7, as one might expect based purely on overall density considerations. As with triggered star formation, however, spontaneous star formation along the midplane cannot account for all of the cluster formation in the cloud. In particular, it cannot explain the formation of the two lowest latitude clusters, numbers 1 and 3, located far from the midplane.

These results suggest that there may be more than one way to form clusters in molecular clouds. Information on cluster ages, obtained from higher resolution *J*, *H*, and *K*

imaging than was possible with SQIID, should provide information on possible age gradients within the cloud, as well as help to clarify the role that triggered or sequential star formation plays in cluster formation.

## 5. SUMMARY

This first reconnaissance of the 155 fields comprising our *JHK* survey of the Rosette Molecular Cloud has revealed seven embedded star clusters. All of the clusters are associated with *IRAS* sources and massive  $^{13}\text{CO}$  molecular clumps. Not all massive molecular clumps (63%–85%) or *IRAS* sources (60%) have associated clusters.

The molecular clumps that contain clusters tend to be among the most massive in the cloud, indicating that high-mass regions are required for the formation of clusters. The presence of a large fraction of high-mass molecular clumps without cluster formation indicates that high mass is a necessary—but not sufficient—condition for cluster formation. The proximity of the cluster-forming clumps to the expanding H II region associated with the OB association, NGC 2244, suggests that increased density of cluster-forming cores, brought about by external compression, may account for the higher star formation efficiencies. However, the presence of at least one cluster far from the ionization front makes it difficult to ascertain the degree to which triggered or sequential star formation is occurring, and whether more than one mechanism may be at work in the formation of clusters in the RMC.

We would like to thank Leo Blitz, Jonathan Williams, Russ Shipman, and Harold Butner for insightful discussions. We would also like to thank Jonathan Williams for providing tables of clump masses and the CO map presented in Figure 2, Jim Morgan for help in the preparation of figures, and the referee, David Block, for his useful suggestions and generous contribution of a photograph that proved useful in our interpretations. R. L. P. would like to thank Frank Clark and Steve Price for their assistance during the early portions of this research, while R. L. P. was at Phillips Laboratory. E. A. L. acknowledges support from NSF grant AST-9314847 and a Hubble Fellowship, grant HF-1047.0193, awarded by Space Telescope Science Institute, which is operated by the Association of Universities for Research in Astronomy, Inc., for NASA under contract NAS 5-26555. The digitized sky survey was produced at the Space Telescope Science Institute under grant NAG W-2166.

## REFERENCES

- Blaauw, A. 1964, *ARA&A*, 2, 213  
 Blitz, L., & Stark, A. A. 1986, *ApJ*, 300, L89  
 Blitz, L., & Thaddeus, P. 1980, *ApJ*, 241, 676  
 Block, D. L. 1990, *Nature*, 247, 452  
 Block, D. L., Dyson, J. E., & Madsen, C. 1992, *ApJ*, 390, L13  
 Block, D. L., Geballe, T. R., & Dyson, J. E. 1993, *A&A*, 273, L41  
 Carpenter, J. M., Snell, R. L., Schloerb, F. P., & Strutskie, M. F. 1993, *ApJ*, 407, 657  
 Cox, P., Deharveng, L., & Leene, A. 1990, *A&A*, 230, 181  
 Elmegreen, B. G., & Lada, C. J. 1977, *ApJ*, 214, 725  
 Gomez, M., Hartmann, L., Kenyon, S. L., & Hewitt, R. 1993, *AJ*, 105, 1927  
 Hanson, M. M., Geballe, T. R., Conti, P. S., & Block, D. L. 1993, *A&A*, 273, L44  
 Kuchar, T. A., & Bania, T. M. 1993, *ApJ*, 414, 664  
 Lada, C. J., Lada, E. A., & Bally, J. 1996, in preparation  
 Lada, C. J., Lada, E. A., Clemens, D. P., & Bally, J. 1994, *ApJ*, 429, 694  
 Lada, C. J., & Lada, E. A. 1991, *ASP Conf. Ser.* 13, *The Formation and Evolution of Star Clusters*, ed. K. A. Janes (San Francisco: ASP), 3  
 Lada, E. A. 1992, *ApJ*, 393, L25  
 Lada, E. A., DePoy, D. L., Evans, N. J., & Gatley, I. 1991, *ApJ*, 371, 171  
 Lada, E. A., Evans, N. J., & Falgarone, E. 1996, *ApJ*, submitted  
 Lada, E. A., & Lada, C. J. 1995, *AJ*, 109, 1682  
 Lada, E. A., Strom, K. M., & Myers, P. C. 1993, in *Protostars and Planets III*, ed. E. H. Levy & J. I. Lunine (Tucson: Univ. Arizona Press), 245  
 Patel, N. A., Xie, T., & Goldsmith, P. F. 1993, *ApJ*, 413, 593  
 Perez, M. R., The, P. S., & Westerlund, B. E. 1987, *PASP*, 99, 1050  
 Phelps, R. L. 1994, in *The Nature and Evolutionary Status of Herbig Ae/Be Stars*, ed. P. S. The, M. R. Perez, & P. J. van den Heuvel (San Francisco: ASP), 339  
 Strom, K. M., Strom, S. E., & Merrill, K. M. 1993, *ApJ*, 412, 233  
 Williams, J., Blitz, L., & Stark, A. 1995, *ApJ*, 451, 252  
 Zinnecker, et al. 1993, in *Protostars and Planets III*, ed. E. H. Levy & J. I. Lunine (Tucson: Univ. Arizona Press), 429